Spin Switching

DOI: 10.1002/ange.201408966

A Two-in-one Pincer Ligand and its Diiron(II) Complex Showing Spin State Switching in Solution through Reversible Ligand Exchange**

*Subhas Samanta, Serhiy Demesko, Sebastian Dechert, and Franc Meyer**

Abstract: *A novel pyrazolate-bridged ligand providing two {PNN} pincer-type compartments has been synthesized. Its diiron(II) complex $LFe_2(OTf)_3(CH_3CN)$ (**1**; Tf = triflate) features, in solid state, two bridging triflate ligands, with a terminal triflate and a MeCN ligand completing the octahedral coordination spheres of the two high-spin metal ions. In MeCN solution, **1** is shown to undergo a sequential, reversible, and complete spin transition to the low-spin state upon cooling. Detailed UV/Vis and ^{19}F NMR spectroscopic studies as well as magnetic measurements have unraveled that spin state switching correlates with a rapid multistep triflate/MeCN ligand exchange equilibrium. The spin transition temperature can be continuously tuned by varying the triflate concentration in solution.*

The spin crossover (SCO) phenomenon has received widespread attention in transition metal chemistry.[1] It is most frequently observed for iron(II) complexes, and its relevance ranges from the role of metal ions in biology[2] to magnetic device applications.[3] Spin crossover is mostly observed for bulk materials in the solid state, in which intermolecular cooperative effects play important roles for achieving complete, often abrupt, and in some cases even hysteretic high-spin/low-spin transitions in response to external perturbations, such as irradiation with light or changes in temperature or pressure.[4,5] In contrast, spin transitions of molecules in solution are relatively rare, and they are usually characterized by gradual SCO following a Boltzmann distribution and resulting in a spin state equilibrium because of the lack of any cooperativity.[6–8] As a consequence, in many cases spin transitions in solution are not complete within the phase limitations of the solvent. In addition to genuine SCO, which does not involve any first sphere ligation changes, spin state sensitivity in solution may arise from changes in the metal ion's chemical environment, for example from ligand dissociation or substitution reactions, or from triggering events in the second coordination sphere.[6,7] In few cases, spin state variations have been associated with reversible solvent binding or with reversible substitution of solvent ligands by weakly coordinating anions.[9,10] Spin state switching in solution has thus been discussed for solution-based chemosensing or MRI contrast applications.[7] As a prominent example, Herges and Tuczek et al. recently developed a porphyrin-based nickel(II) system that shows magnetic bistability in solution, induced by the light-driven reversible coordination of a tethered ligand to the nickel ion.[11]

Here we report a diiron(II) complex that undergoes a reversible and essentially complete high-spin/low-spin transition in solution through a multistep temperature-dependent ligand exchange reaction. The diiron(II) complex is based on a novel type of binucleating ligand scaffold that is composed of two {PNN} pincer-type subunits, and that can be viewed as a dinucleating version of the bipyridine-based {PNN} pincer ligand **I** (Scheme 1).[12,13] Complexes with

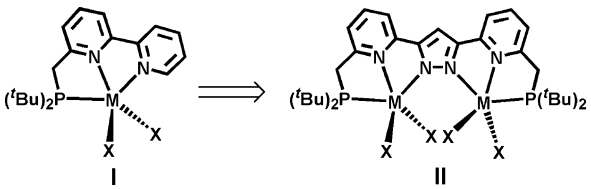

Scheme 1. Complexes **I** with {PNN} pincer ligand and pyrazolate-bridged binuclear systems **II** with two pincer-type {PNN} subunits.

tridentate pincer ligands are currently receiving much attention,[14] and the new ligand was designed to allow for cooperativity effects in chemical transformations mediated by two adjacent metal ions that are hosted in pincer-type binding pockets. To this end the pincer motif was merged with a pyrazolate bridging unit (**II**); compartmental pyrazolate-based ligands with chelating side arms in the 3- and 5-positions of the heterocycle have indeed been used beneficially for achieving bimetallic reactivity,[15] and also for inducing cooperativity and multistability in oligonuclear SCO complexes.[16,17]

The preparation of the new proligand HL was achieved through a two-step phosphorylation of the previously reported[18] 3,5-bis(6-methylpyridyl-2-yl)pyrazole (**A**, Scheme 2); details of the synthetic procedure are provided in the Supporting Information (SI). In the first step, deprotonation of **A** by *n*BuLi (2.5 equiv) followed by the addition of di(*tert*-butyl)chlorophosphine (1 equiv) resulted in the formation of **B** in 90% yield. Repeating the sequence with 4.5 equivalents of *n*BuLi for deprotonation in the second step followed by the addition of another equivalent of di(*tert*-butyl)chlorophosphine gave the desired proligand HL in 42%

[*] Dr. S. Samanta, Dr. S. Demesko, Dr. S. Dechert, Prof. Dr. F. Meyer
Institut für Anorganische Chemie
Georg-August-Universität Göttingen
Tammannstrasse 4, 37077 Göttingen (Germany)
E-mail: franc.meyer@chemie.uni-goettingen.de
Homepage: http://www.meyer.chemie.uni-goettingen.de

[**] S.S. is grateful to the Alexander von Humboldt foundation for postdoctoral fellowship support. This work has been carried out in the framework of the European COST action CM 1305 (ECOSTBIO).

Supporting information for this article is available on the WWW under http://dx.doi.org/10.1002/anie.201408966.

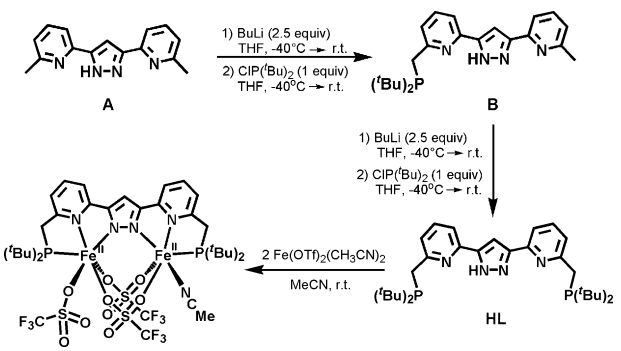

Scheme 2. Preparation of proligand HL from **A** and reaction of HL with $Fe(OTf)_2(CH_3CN)_2$ to form complex **1**.

yield. A two-fold phosphorylation of **A** in a single-step procedure proved unsuccessful.

The constitution of HL was confirmed by single-crystal X-ray diffraction (see SI). The ^{1}H NMR spectrum of HL in [D$_6$]acetone solution shows a characteristic sharp singlet at 7.4 ppm for the pyrazole-H[4], but otherwise broadened resonances that sharpen upon lowering the temperature, likely because of tautomerism of the pyrazole-NH. In line with this result, the ^{31}P NMR spectrum at 253 K shows two signals at 35.6 and 34.8 ppm that coalesce at around 323 K (see Figures S1–S4).

Reaction of HL with two equivalents of $Fe(OTf)_2(CH_3CN)_2$ (OTf = triflate) in acetonitrile and in the presence of 10 equivalents of NEt_3 (for capturing the pyrazole-N-bound proton) gave a reddish yellow solution from which light yellow crystalline $LFe_2(OTf)_3(CH_3CN)$ (**1**) could be isolated in 60% yield. **1** is an air sensitive complex that is soluble in common organic solvents. The electrospray ionization mass spectrum (ESI-MS) of an acetonitrile solution of **1** shows a dominant peak at m/z 948 amu corresponding to the ion $[M-OTf^- - CH_3CN]^+$, suggesting that some triflate ions remain associated with the $[LFe_2]^{3+}$ scaffold in solution, but that both triflate and MeCN ligands are labile.

Compound **1** was characterized by X-ray diffraction analysis. The molecular structure is shown in Figure 1, and structural parameters are provided in the SI (Tables S1–S3).

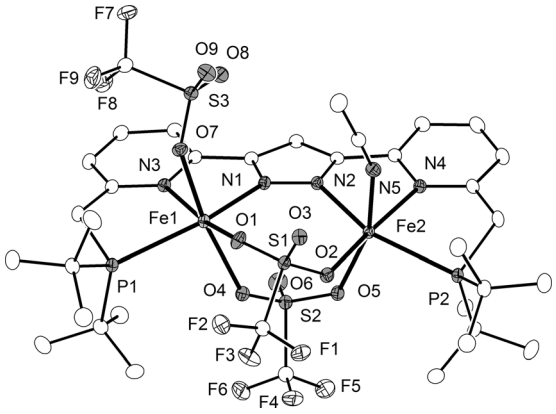

Figure 1. Molecular structure of **1** at 133 K determined by X-ray diffraction (30% probability thermal ellipsoids). Hydrogen atoms are omitted for clarity.

In the solid state, **1** features a distorted octahedral geometry for both ferrous ions. Each of the pincer cavities binds an iron atom in a meridional fashion along with two triflate counterions that serve as bridges within the bimetallic pocket. The coordination environment is completed by a terminal triflate at Fe1 and an acetonitrile molecule at Fe2. Overall, this represents an unsymmetrical binuclear complex with two pincer-type subunits, and with weak and potentially labile ligands filling all remaining coordination sites.

A Mößbauer spectrum of solid **1** at 80 K (Figure 2, top) shows two closely spaced doublets with isomer shifts of 1.15 and 1.18 mm s^{-1} and large quadruple splittings ΔE_Q of 3.20 and 3.53 mm s^{-1}, respectively, in accordance with two ferrous

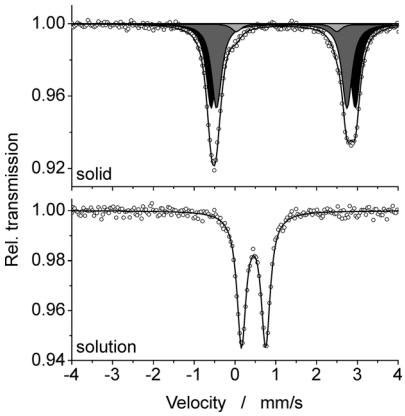

Figure 2. Mößbauer spectra of **1** in the solid state (top) and in frozen MeCN solution (bottom) at 80 K.

ions in slightly different environment,[19] as was found crystallographically. Variable temperature magnetic susceptibility data confirm the high-spin Fe^{II} configuration (Figure 3, left). The decrease of $\chi_M T$ at very low temperatures likely reflects weak intramolecular antiferromagnetic exchange and zero-field splitting (a simulation gave $g = 2.16$, $J = -0.2$ cm^{-1}, $|D| = 5.7$ cm^{-1}; see SI for details).

Resonances of **1** in the ^{1}H NMR spectrum in CD_3CN at room temperature are broadened and paramagnetically shifted (Figure S5). Though it was not possible to assign all

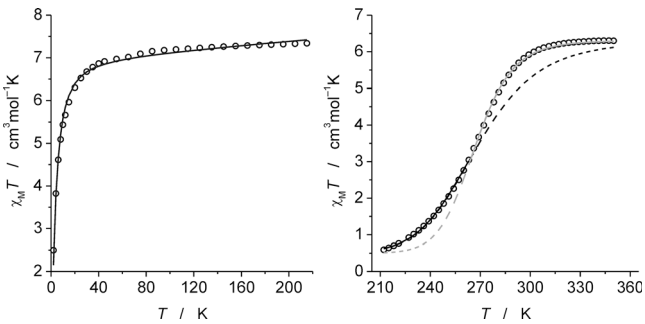

Figure 3. Variable temperature magnetic susceptibility of **1** determined by SQUID magnetometry. Left: in solid state; the black line represent the simulation (see SI for details); Right: in MeCN solution; the gray line represents the simulation in the range 350–263 K; the black line represents the simulation from 263–212 K (see text for details).

protons, the broad singlet signal for a large number of protons at 8.1 ppm can be unambiguously attributed to the *tert*-butyl groups of the ligand scaffold in the complex. Surprisingly, upon cooling the paramagnetically shifted resonances gradually disappear and the broad signal for the *tert*-butyl groups undergoes a shift to higher field, with a final chemical shift of 1.8 ppm at 238 K; the latter chemical shift is indicative of a diamagnetic compound at that temperature. This observation prompted to collect Mößbauer data of **1** in frozen MeCN solution at 80 K (Figure 2, bottom). Under those conditions the spectrum shows a single narrow quadrupole doublet with an isomer shift of 0.46 mm s^{-1} and $\Delta E_Q = 0.59$ mm s^{-1} characteristic for a low-spin iron(II) complex.[19] Both ^{1}H NMR and Mößbauer data thus suggest that an almost complete temperature-induced spin state change of the complex occurs in MeCN solution, and that both ferrous ions have identical coordination environments at low temperatures.

At room temperature in MeCN solution, compound **1** shows intense UV/Vis absorptions at 261 nm (ε = 21 700 M^{-1}cm^{-1}) and 308 nm (ε = 20 800 M^{-1}cm^{-1}; Figure 4).

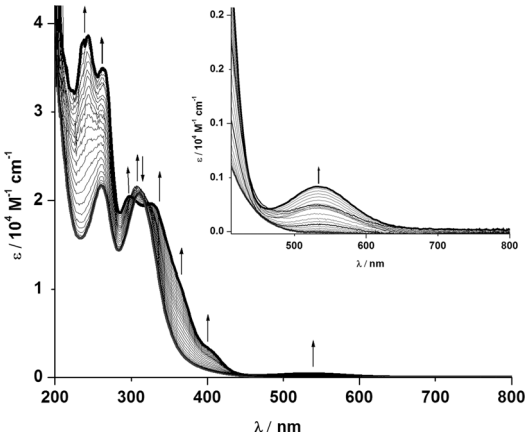

Figure 4. Variable temperature UV/Vis spectral changes upon cooling from 323 K to 233 K in acetonitrile solution (conc. 4.5×10^{-4} M).

These UV/Vis bands are tentatively assigned to metal-to-ligand charge transfer (MLCT) and intraligand transitions. Upon cooling to 233 K the solution color changes from pale yellow to intense red, and the UV/Vis spectrum shows drastic changes. Most prominently, absorptivity in the high-energy region increases with the generation of two intense bands at 263 nm (ε = 35 300 M^{-1}cm^{-1}) and 241 nm (ε = 38 900 M^{-1}cm^{-1}). Notably, low-spin iron(II) with its filled t_{2g} set of orbitals and singlet electronic state is expected to feature more intense MLCT transitions. In addition a shoulder at 409 nm and a weak band at 529 nm (ε = 374 M^{-1}cm^{-1}) arises upon cooling, likely attributable to d–d transitions.[10,20] More detailed spectral monitoring of the solution, in particular in the 285–350 nm region, suggests a reversible multistep transformation (at least two steps) upon varying the temperature, with an intermediate predominating at around 270 K (Figures 5 and S7c). It should be noted that solutions of **1** in other solvents such as acetone or THF do not show any such temperature-dependent changes.

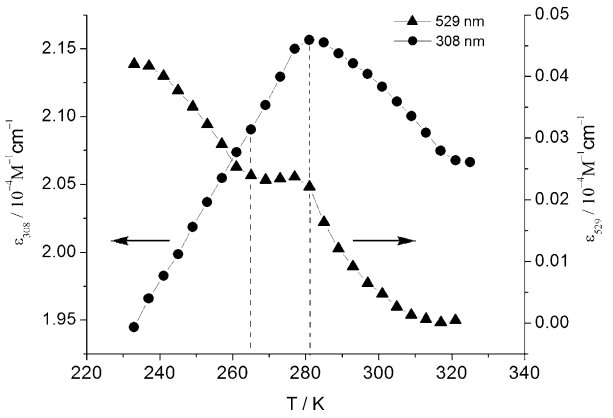

Figure 5. Variable-temperature UV/Vis spectral changes at 529 nm and 308 nm.

We surmised that ligand exchange, namely the substitution of triflates by MeCN, takes place in solution upon lowering the temperature. MeCN exhibits a stronger ligand field and induces the switch to the low-spin state. To corroborate this assumption, variable temperature ^{19}F NMR spectra in [D$_3$]MeCN solution were recorded. At 323 K a single relatively broad ^{19}F NMR signal is observed at −22.8 ppm, indicating a rapid exchange of the bridging and terminal triflates on the NMR time scale. Upon cooling, the signal broadens further with a concomitant shift to higher fields (see the upper ten spectra from 323–238 K in Figure 6).

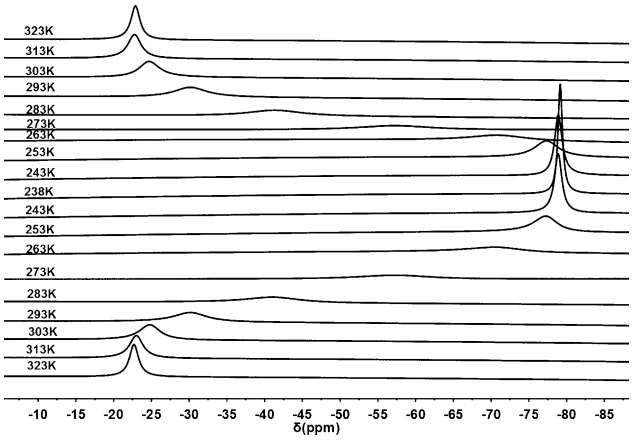

Figure 6. Variable-temperature ^{19}F NMR spectra of the complex **1** in acetonitrile. Spectra from the top are on cooling from 323 to 238 K and then on subsequent warming from 238 to 323 K.

These changes suggest rapid exchange equilibria of triflates and MeCN ligands. Below 253 K the ^{19}F NMR signal becomes sharp again, and it is finally found at −79.2 ppm at 238 K. Notably this $\delta(^{19}F)$ chemical shift corresponds to uncoordinated triflate, because NaOTf in MeCN solution shows an essentially identical ^{19}F NMR resonance (−79.4 ppm). These changes are fully reversible upon warming (see the lower nine spectra from 243–323 K in Figure 6). Careful evaluation of the temperature dependence of the ^{19}F NMR chemical shift suggests a three-step process, with the slope of the $\delta(^{19}F)$ versus T curve changing at around 283 K and 263 K (Fig-

ure S9). This likely reflects the sequential dissociation of the three triflates and is fully in accordance with the UV/Vis results.

Variable temperature magnetic susceptibility measurements were performed by both Evans method[21] as well as SQUID magnetometry (SQUID = superconducting quantum interference device) for complex **1** in MeCN solution, which allows following the changes of its magnetic moment. Results obtained using the two methods are consistent (Figure S9); SQUID data are depicted in Figure 3 (right side) and reveal almost complete spin state switching and transformation to the low-spin iron(II) complex at 212 K. Magnetic data are fully congruent when measured in cooling and heating modes, indicating full reversibility of the spin transition process. Comparison of the temperature dependence of the ^{19}F NMR data, which reflect the ligand exchange processes, and the changes of the magnetic moment are consistent, thereby indicating that the spin transition is indeed correlated with the ligand exchange reactions. Thermodynamic parameters of the SCO transition were calculated according to[22,23]

$$\gamma = \frac{1}{1+\exp(\Delta H/RT - \Delta S/R)} \quad (1)$$

in which ΔH and ΔS are the enthalpy and entropy parameters, and R is the universal gas constant. It turned out that simulation of the complete temperature range with only one set of parameters does not give a good overall fit. However, good agreement with experimental data was found for the temperature range 350 to 263 K with parameters $\Delta H = 52.6\ \mathrm{kJ\,mol^{-1}}$ and $\Delta S = 197\ \mathrm{J\,mol^{-1}\,K^{-1}}$ (gray line in Figure 3, right side), and for the temperature range 263 to 212 K with parameters $\Delta H = 32.4\ \mathrm{kJ\,mol^{-1}}$ and $\Delta S = 121\ \mathrm{J\,mol^{-1}\,K^{-1}}$ (black line in Figure 3, right side). Therefore, simulation of the magnetic data suggests a two-step spin switching phenomenon, in which the first step is completed at around 263 K. Notably the experimental value of $\chi_M T$ at 263 K matches with the one expected for a situation with one low-spin iron(II) and one high-spin(II) ion in the complex (LS–HS, 3.15 $\mathrm{cm^3\,mol^{-1}\,K}$). The large experimental values for ΔH and ΔS, in particular for the step at higher temperatures, are beyond the typical range for genuine SCO without any dissociation or exchange of ligands (usually $\Delta H < 30\ \mathrm{kJ\,mol^{-1}}$ and $\Delta S < 130\ \mathrm{J\,mol^{-1}\,K^{-1}}$).[6,7] Combining the results from variable temperature UV/Vis, ^{19}F NMR spectroscopy, and magnetic susceptibility measurements thus suggests that spin state switching of one ferrous ion occurs above 263 K and is associated with the substitution of two triflate ligands by MeCN, whereas substitution of the third triflate proceeds below 263 K and causes spin state switching of the second ferrous ion to give the LS–LS species.

To further substantiate the presence of a ligand exchange equilibrium inducing the spin transition, variable temperature magnetic susceptibility data were measured for different triflate ion concentrations in solution after adding 6, 12, 18, 24, and 30 equiv of NaOTf. Due to the fact that data obtained by SQUID measurements and Evans method gave essentially identical results in the above studies, the latter was used for these experiments. Data have been collected down to 238 K to avoid freezing of the solution. Plots of the variable temperature χT data for different concentrations of NaOTf are shown in Figure 7.

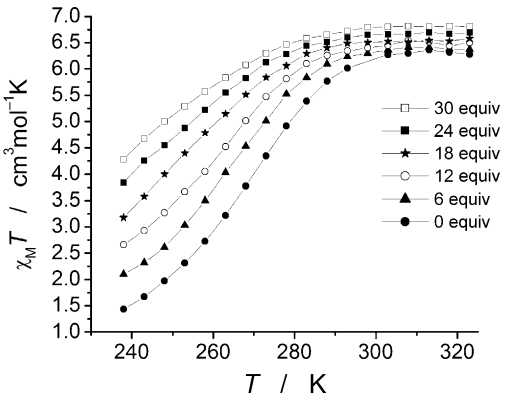

Figure 7. Temperature dependence of $\chi_M T$ for **1** in MeCN solution with different equivalents of NaOTf added.

It is evident that the spin state transition shifts to lower temperatures with increasing NaOTf concentration, which is in line with the above discussion: the ligand exchange equilibrium is shifted toward the high-spin species with bound triflate in the presence of a high triflate loading. Furthermore the magnetic moment at 320 K slightly increases with increasing triflate concentration, indicating that neat **1** (without added NaOTf), because of the equilibrium in solution, is only around 96 % in the high-spin state at that temperature. Plots of the percentage of molecules in their high-spin state at different temperatures and different triflate concentrations are shown in Figure S9. The results confirm that the triflate/MeCN ligand exchange is directly associated with the spin state switching process (Scheme 3).

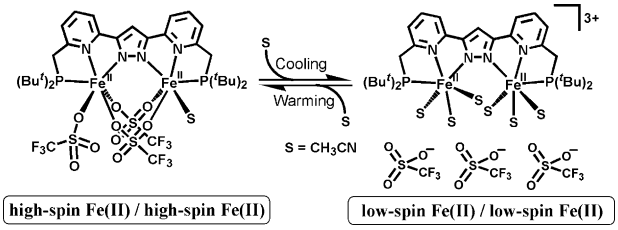

Scheme 3. Triflate/MeCN ligand exchange and spin state switching.

In conclusion, a novel pyrazolate-bridged ligand with two tridentate pincer-type {PNN} compartments is presented. Its diiron(II) complex $LFe_2(OTf)_3(CH_3CN)$ (**1**), which in the solid state is found in the all-high-spin configuration (HS–HS), is shown to undergo reversible and complete spin state switching in MeCN solution, which has been rationalized on the basis of a temperature-dependent triflate/MeCN ligand exchange equilibrium. Thorough analysis of variable temperature UV/Vis spectroscopy, ^{19}F NMR spectroscopy, and magnetic susceptibility data have elucidated a sequential two-step spin transition process that correlates with the

substitution, by MeCN ligands, of two triflates (in the first step) and of the third triflate (in the second step) upon lowering the temperature, generating a mixed-spin (LS–HS) species $[LFe_2(OTf)(CH_3CN)_x]^{2+}$ around 263 K and a LS–LS species $[LFe_2(CH_3CN)_y]^{3+}$ at even lower temperatures. Although the spin crossover of iron(II) compounds in the solid state, induced by light or by changes in temperature or pressure, is very well established and heavily studied, systems that undergo complete spin switching in solution are relatively scarce, and spin transitions in solution have rarely been traced back to specific molecular events. One may speculate about potential sensor applications of such bi- and multistable systems, but we find the prospect of tuning chemical reactivity (e.g., the reaction of diferrous complexes with O_2) by temperature-induced spin state changes in solution, such as observed here, a particularly interesting perspective.[24] More generally, in view of the rapidly developing catalytic applications of mononuclear pincer complexes (with a recent emphasis on iron pincer complexes),[13,25] we anticipate exciting chemistry of bimetallic systems with two potentially synergetic pincer-type subunits based on L^- or related ligands.

Received: September 10, 2014
Published online: November 24, 2014

Keywords: diiron complexes · ligand exchange · magnetic properties · pincer ligands · spin crossover

[1] a) P. Gütlich, A. Hauser, H. Spiering, *Angew. Chem. Int. Ed. Engl.* **1994**, *33*, 2024 – 2054; *Angew. Chem.* **1994**, *106*, 2109 – 2141; b) "Spin Crossover in Transition Metal Compounds I – III": *Topics in Current Chemistry*, *Vol. 233 – 235* (Eds.: P. Gütlich, H. A. Goodwin), Springer, Berlin, **2004**; c) K. S. Murray, *Eur. J. Inorg. Chem.* **2008**, 3101 – 3121; d) *Spin-Crossover Materials: Properties and Applications* (Ed.: M. Halcrow), Wiley, Chichester, **2013**.

[2] a) K. P. Kepp, *ChemPhysChem* **2013**, *14*, 3551 – 3558; b) M. Nakamura, Y. Ohgo, A. Ikezaki, in *Handbook of Porphyrin Science*, *Vol. 7* (Eds.: K. M. Kadish, K. M. Smith, R. Guillard), World Scientific, Singapore, **2010**, pp. 1 – 146.

[3] a) G. Molnár, L. Salmon, W. Nicolazzi, F. Terki, A. Bousseksou, *J. Mater. Chem. C* **2014**, *2*, 1360 – 1366; b) A. Grohmann, M. Haryono, K. Student, P. Müller, M. Stocker, *Eur. J. Inorg. Chem.* **2013**, 662 – 669; c) J.-F. Létard, P. Guionneau, L. Goux-Capes, *Top. Curr. Chem.* **2004**, *235*, 221 – 249.

[4] a) G. N. Newton, M. Nihei, H. Oshio, *Eur. J. Inorg. Chem.* **2011**, 3031 – 3042; b) P. Gütlich, A. Hauser, *Coord. Chem. Rev.* **1990**, *97*, 1 – 22.

[5] a) P. Gütlich, A. B. Gaspar, Y. Garcia, *Beilstein J. Org. Chem.* **2013**, *9*, 342 – 391; b) M. A. Halcrow, *Chem. Soc. Rev.* **2011**, *40*, 4119 – 4142.

[6] H. Toftlund, *Monatsh. Chem.* **2001**, *132*, 1269 – 1277.

[7] M. P. Shores, C. M. Klug, S. R. Fiedler in *Spin-Crossover Materials: Properties and Applications* (Ed.: M. A. Halcrow), Wiley, Chichester, **2013**, pp. 281 – 301.

[8] B. Weber, F. A. Walker, *Inorg. Chem.* **2007**, *46*, 6794 – 6803.

[9] K. P. Bryliakov, E. A. Duban, E. P. Talsi, *Eur. J. Inorg. Chem.* **2005**, 72 – 76.

[10] a) A. Diebold, K. S. Hagen, *Inorg. Chem.* **1998**, *37*, 215 – 223; b) D. W. Blakesley, S. C. Payne, K. S. Hagen, *Inorg. Chem.* **2000**, *39*, 1979 – 1989.

[11] a) S. Venkataramani, U. Jana, M. Dommaschk, F. D. Sönnichsen, F. Tuczek, R. Herges, *Science* **2011**, *331*, 445 – 447; b) S. Thies, H. Sell, C. Schütt, C. Bornholdt, C. Näther, F. Tuczek, R. Herges, *J. Am. Chem. Soc.* **2011**, *133*, 16243 – 16250.

[12] a) E. Balaraman, B. Gnanaprakasam, L. J. W. Shimon, D. Milstein, *J. Am. Chem. Soc.* **2010**, *132*, 16756 – 16758; b) P. Hu, Y. Diskin-Posner, Y. Ben-David, D. Milstein, *ACS Catal.* **2014**, *4*, 2649 – 2652.

[13] L. Zhang, D. Peng, X. Leng, Z. Huang, *Angew. Chem. Int. Ed.* **2013**, *52*, 3676 – 3680; *Angew. Chem.* **2013**, *125*, 3764 – 3768.

[14] a) G. van Koten, *J. Organomet. Chem.* **2013**, *730*, 156 – 164; b) C. Gunanathan, D. Milstein, *Acc. Chem. Res.* **2011**, *44*, 588 – 602; c) S. Schneider, J. Meiners, B. Askevold, *Eur. J. Inorg. Chem.* **2012**, 412 – 429; d) O. V. Ozerov in *The Chemistry of Pincer Compounds* (Eds.: D. Morales-Morales, C. M. Jensen), Elsevier, Amsterdam, the Netherlands, **2007**, pp. 287; e) J. I. van der Vlugt, J. N. H. Reek, *Angew. Chem. Int. Ed.* **2009**, *48*, 8832 – 8846; *Angew. Chem.* **2009**, *121*, 8990 – 9004; f) M. Albrecht, G. van Koten, *Angew. Chem. Int. Ed.* **2001**, *40*, 3750 – 3781; *Angew. Chem.* **2001**, *113*, 3866 – 3898, and references therein.

[15] a) J. Klingele, S. Dechert, F. Meyer, *Coord. Chem. Rev.* **2009**, *253*, 2698 – 2741; b) B. Burger, S. Demeshko, E. Bill, S. Dechert, F. Meyer, *Angew. Chem. Int. Ed.* **2012**, *51*, 10045 – 10049; *Angew. Chem.* **2012**, *124*, 10190 – 10195; c) S. Neudeck, S. Maji, I. López, S. Meyer, F. Meyer, A. Llobet, *J. Am. Chem. Soc.* **2014**, *136*, 24 – 27; d) K. E. Dalle, T. Gruene, S. Dechert, S. Demeshko, F. Meyer, *J. Am. Chem. Soc.* **2014**, *136*, 7428 – 7434.

[16] a) K. Nakano, N. Suemura, K. Yoneda, S. Kawata, S. Kaizaki, K. Sumio, *Dalton Trans.* **2005**, 740 – 743; b) A. Slimani, F. Varret, K. Boukheddaden, D. Garrot, H. Oubouchou, S. Kaizaki, *Phys. Rev. Lett.* **2013**, *110*, 087208; c) J. Olguín, S. Brooker, *Coord. Chem. Rev.* **2011**, *255*, 203 – 240.

[17] a) B. Schneider, S. Demeshko, S. Dechert, F. Meyer, *Angew. Chem. Int. Ed.* **2010**, *49*, 9274 – 9277; *Angew. Chem.* **2010**, *122*, 9461 – 9464; b) B. Schneider, S. Demeshko, S. Neudeck, S. Dechert, F. Meyer, *Inorg. Chem.* **2013**, *52*, 13230 – 13237; c) M. Steinert, B. Schneider, S. Dechert, S. Demeshko, F. Meyer, *Angew. Chem. Int. Ed.* **2014**, *53*, 6135 – 6139; *Angew. Chem.* **2014**, *126*, 6249 – 6253.

[18] J. Pons, X. López, E. Benet, J. Casabo, *Polyhedron* **1990**, *9*, 2839 – 2845.

[19] P. Gütlich, E. Bill, A. X. Trautwein, *Mössbauer Spectroscopy and Transition Metal Complexes*, Springer, Heidelberg, **2011**.

[20] N. Ortega-Villar, A. L. Thompson, M. C. Muñoz, V. M. Ugalde-Saldívar, A. E. Goeta, R. Moreno-Esparza, J. A. Real, *Chem. Eur. J.* **2005**, *11*, 5721 – 5734.

[21] E. M. Schubert, *J. Chem. Ed.* http://pubs.acs.org/doi/pdfplus/10.1021/ed069p62.1.

[22] O. Kahn, *Molecular Magnetism*, VCH Publishers, New York, **1993**.

[23] M. Sorai, S. Seki, *J. Phys. Chem. Solids* **1974**, *35*, 555.

[24] a) T. Kojima, Y. Hirai, T. Ishizuka, Y. Shiota, K. Yoshizawa, K. Ikemura, T. Ogura, S. Fukuzumi, *Angew. Chem. Int. Ed.* **2010**, *49*, 8449 – 8453; *Angew. Chem.* **2010**, *122*, 8627 – 8631; b) S. Ye, C.-Y. Geng, S. Shaik, F. Neese, *Phys. Chem. Chem. Phys.* **2013**, *15*, 8017 – 8030.

[25] See for example: a) P. Bhattacharya, H. Guan, *Comments Inorg. Chem.* **2011**, *32*, 88 – 112; b) K. L. Fillman, E. A. Bielinski, T. J. Schmeier, J. C. Nesvet, T. M. Woodruff, C. J. Pan, M. K. Takase, N. Hazari, M. L. Neidig, *Inorg. Chem.* **2014**, *53*, 6066 – 6072; c) P. Ghosh, S. Samanta, S. K. Roy, S. Demeshko, F. Meyer, S. Goswami, *Inorg. Chem.* **2014**, *53*, 4678 – 4686; d) I. Koehne, T. J. Schmeier, E. A. Bielinski, C. J. Pan, P. O. Lagaditis, W. H. Bernskoetter, M. K. Takase, C. Würtele, N. Hazari, S. Schneider, *Inorg. Chem.* **2014**, *53*, 2133 – 2143.

